9-10-91
E6476

NASA Technical Memorandum 105179
ICOMP-91-13; CMOTT-91-4

A Comparison of Numerical Methods for the Rayleigh Equation in Unbounded Domains

W.W. Liou
Institute for Computational Mechanics in Propulsion
and Center for Modeling of Turbulence and Transition
Lewis Research Center
Cleveland, Ohio

and

P.J. Morris
Pennsylvania State University
University Park, Pennsylvania

August 1991

INSTITUTE FOR COMPUTATIONAL MECHANICS IN PROPULSION
NASA
LEWIS RESEARCH CENTER
ICOMP
CASE WESTERN RESERVE UNIVERSITY

NASA

A COMPARISON OF NUMERICAL METHODS FOR THE RAYLEIGH EQUATION IN UNBOUNDED DOMAINS

W.W. Liou
Institute for Computational Mechanics in Propulsion
and Center for Modeling of Turbulence and Transition
Lewis Research Center
Cleveland, Ohio 44135

P.J. Morris
Pennsylvania State University
Department of Aerospace Engineering
University Park, Pennsylvania 16802

SUMMARY

A second-order finite difference and two spectral methods including a Chebyshev tau and a Chebyshev collocation method have been implemented to determine the linear hydrodynamic stability of an unbounded shear flow. The velocity profile of the basic flow in the stability analysis mimicks that of a one–stream free mixing layer. Local and global eigenvalue solution methods are used to determine individual eigenvalues and the eigenvalue spectrum, respectively. The calculated eigenvalue spectrum includes a discrete mode, a continuous spectrum associated with the equation singularity and a continuous spectrum associated with the domain unboundedness. The efficiency and the accuracy of these discretization methods in the prediction of the eigensolutions of the discrete mode have been evaluated by comparison with a conventional shooting procedure. Their capabilities in mapping out the continuous eigenvalue spectra are also discussed.

1. INTRODUCTION

This paper studies the numerical solutions of a boundary value problem using four different solution methods. The Rayleigh equation[1] governs the inviscid instability properties of linearized disturbances. With the conventional normal mode representations for disturbances, the equation for the complex amplitude, $\hat{v}$, of the velocity perturbation in the y-direction is

$$\left\{ (\alpha U - \omega) \left(\frac{\mathrm{d}^2}{\mathrm{d}y^2} - \alpha^2 \right) - \alpha \frac{\mathrm{d}^2 U}{\mathrm{d}y^2} \right\} \hat{v} = 0 \tag{1}$$

In a spatial analysis, it is assumed that the disturbances with real frequency, ω, traveling at the speed, ω/α_r, are amplified at the rate $\exp(-\alpha_i x)$ upon the basic parallel flow described by the mean velocity in the x-direction , $U(y)$. α denotes the complex wavenumber and ω the frequency. The Rayleigh equation, together with the boundary conditions

$$\hat{v} \to 0 , \qquad y \to \pm \infty \tag{2}$$

defines the basic linear inviscid instability problem, in the form of a boundary value problem for parallel free shear flows in an unbounded domain. Thus we are solving an eigenvalue problem to determine the dispersion relationship

$$\alpha = \alpha (\omega) \tag{3}$$

Traditionally, the hydrodynamic stability problem has been solved by shooting techniques[2]. This involves the solution of two initial value problems with the two boundary conditions as their respective initial conditions. Eigenvalues are determined by satisfying a matching condition at a certain intermediate point or boundary in the flow. A good knowledge of the characteristics of the solutions is often needed in the shooting technique in order to make a good initial guess for the eigenvalues. Also, the accuracy of the solutions is often limited by the accuracy of the numerical integration scheme.

Recently, interest in the application of spectral approximation methods has grown in all branches of science and engineering. Spectral methods are useful in problems where high resolution is required[3,4]. These methods have also been studied in classical problems of computational fluid dynamics[5,6] and in turbulence simulations[7]. Canuto et al.[8] have given a detailed description of the technical aspects of the applications of various spectral methods in fluid dynamics.

Another application of spectral methods has been in the solution of hydrodynamic stability problems. For example, Orszag[9] compared spectral methods based on different expansion polynomials and used a Chebyshev polynomial expansion to study the temporal instability of plane Poiseuille flow. When this discretization is applied to the linearized equations of hydrodynamic stability with the appropriate boundary conditions, an algebraic eigenvalue problem is obtained. For temporal instability, in which a fixed wavelength disturbance grows or decays in time, the complex frequency is the eigenvalue. This parameter appears linearly in the problem and standard algebraic eigenvalue techniques may be used to determine the eigenvalues. However, most shear driven instabilities are spatially unstable. In this case a disturbance of fixed real frequency grows or decays in space, and the complex wavenumber of the disturbance is the eigenvalue. The wavenumber appears nonlinearly in the problem and standard algebraic eigenvalue techniques are not applicable. Bridges and Morris[10] showed that the Linear Companion Matrix Method (LCM) and a method based on matrix factorization (MF) could be applied successfully to this problem. The LCM approximates the entire eigenvalue spectrum. The factorization method gives only a subset of the eigenvalue spectrum. However, the size of the companion matrix in the LCM is p times that of the original matrices where p is the order to which the eigenvalue appears. Note that neither of the two methods requires initial guesses for eigenvalue calculations.

So far the applications of the spectral approximations in conjunction with the global eigenvalue solution methods have been limited to the boundary layer or bounded shear flow instability problem[10,11]. In the present analysis, two spectral methods, the Chebyshev tau method and a Chebyshev collocation method are used to determine the spatial, inviscid stability of a free shear layer. The resulting eigenvalue problem in which the parameter appears nonlinearly is solved using the LCM and MF.

Moreover, the advent of these computational methods, LCM and MF, has made it feasible to solve the spatial stability problem using other discretization techniques, such as finite difference formulation. The application of the finite difference techniques also results in an eigenvalue problem in which the parameter appears nonlinearly. Therefore, standard algebraic eigenvalue techniques are not applicable in this case as well and the global eigenvalue solution methods have to be used as in the case of spectral approximations. For both spectral and finite difference discretizations, the accuracy of the solutions depends mainly on the order of approximations. In the present analysis, the order of approximation is measured by either the number of Chebyshev polynomials used in the spectral methods or the number of grid points at which differential equations are discretized in the finite difference formulation. Finite difference discretizations, however, are much simpler to implement than spectral methods. Therefore, the finite difference approximations provide a viable alternative for hydrodynamic stability analyses using the global eigenvalue solution methods.

In the present paper two spectral approximations are used to determine the spatial, inviscid stability of a two-dimensional free shear layer. A simple finite difference scheme is also considered. The solutions are compared with that using the shooting procedure. This stability analysis is of interest as experimental observations[12,13] have shown that the local characteristics of large–scale coherent, turbulent structures in free mixing layers are described remarkably well as inviscid instability waves. If these observations are to form the basis of a turbulence model it is valuable to have efficient numerical schemes to solve the inviscid hydrodynamic stability problem. Liou[14] has successfully implemented these global approximation schemes in developing turbulence models based on a linear theory to simulate the evolution of a turbulent free mixing layer.

In the following sections, the basic boundary value problem, the numerical discretizations and the eigenvalue solutions are first described. Comparisons of the accuracy and efficiency of the schemes are then given. The various features of the eigenvalue spectrum of the Rayleigh equation unveiled by the global numerical approximations are also discussed.

2. FORMULATION

A transformation

$$z = f(y) \tag{4}$$

which maps the unbounded physical domain onto the finite Chebyshev domain [-1,1] must be used to apply the Chebyshev spectral methods. The transformed Rayleigh equation becomes

$$[U\hat{v}]\alpha^3 - [\omega\hat{v}]\alpha^2 - [\,U\,(\,\hat{v}'m\,)'\,m - (U'm\,)'\,m\hat{v}\,]\,\alpha + \omega\,(\,\hat{v}'m\,)'\,m = 0 \tag{5}$$

where m denotes the metric of the transformation and $(\quad)'$ denotes d/dz. The boundary conditions become

$$\hat{v} \to 0\,, \qquad z \to \pm 1 \tag{6}$$

For the Rayleigh equation, it is shown below that the system of equations generated by each of the three approximation methods forms an eigenvalue problem with the eigenvalue, α, appearing nonlinearly. That is,

$$D_3(\alpha)\mathbf{v} = 0 \tag{7}$$

where

$$D_3(\alpha) = \mathbf{C}_0\alpha^3 + \mathbf{C}_1\alpha^2 + \mathbf{C}_2\alpha + \mathbf{C}_3.$$

The $\mathbf{C}_0, \mathbf{C}_1, \mathbf{C}_2$ and $\mathbf{C}_3$ are the coefficient matrices of the lambda matrix $D_3(\alpha)$. The components of the eigenvector $\mathbf{v}$ are either the expansion coefficients of the

Chebyshev series approximation or the solution vectors themselves. The eigenvalues of the system are the roots of the characteristic equation

$$\det\left|D_3(\alpha)\right| = 0 \tag{8}$$

2.1 Chebyshev Tau Method

In the Chebyshev tau (CT) method the solution $\hat{v}$ is approximated by a truncated finite series expansion of Chebyshev polynomials,

$$\hat{v}(z) \simeq \mathbf{v}(z) = \frac{v_0}{2} + \sum_{n=1}^{N} v_n\, T_n(z) \tag{9}$$

where $T_n(z)$ is the n^{th} order Chebyshev polynomial of the first kind. The various properties of Chebyshev polynomials can be found in Fox and Parker[15]. For convenience the Rayleigh equation is now written in integral form:

$$\hat{A}\alpha^3 + \hat{B}\alpha^2 + \hat{C}\alpha + \hat{D} + b_1 z + b_2 = 0 \tag{10}$$

where

$$\hat{A} = \int\!\!\int U\hat{v}\ dzdz,$$

$$\hat{B} = -w\int\!\!\int \hat{v}\ dzdz,$$

$$\hat{C} = -m^2U\hat{v} + \frac{3}{2}\int (m^2)'U\hat{v}\ dz + 2\int m^2U'\hat{v}\ dz -$$

$$\int\!\!\int \left(\frac{m^2}{2}\right)''U\hat{v}\ dzdz - \int\!\!\int (m^2)'U'\hat{v}\ dzdz,$$

$$\hat{D} = w\ \{m^2\hat{v} - \frac{3}{2}\int (m^2)'\hat{v}\ dz + \int\!\!\int \left(\frac{m^2}{2}\right)''\hat{v}\}\ dzdz,$$

and b_1, b_2 are integration constants. The series representation of $v(z)$ is substituted into equation (10) and the integrations are performed by making use of the Chebyshev relations

$$\int T_n(z)\ dz = \begin{cases} T_1(z) & n = 0 \\ \frac{1}{4}[T_0(z) + T_2(z)] & n = 1 \\ \frac{T_{n+1}(z)}{2(n+1)} - \frac{T_{n-1}(z)}{2(n-1)} & n \geq 2 \end{cases} \tag{11}$$

After the application of the above expressions to the integrated Rayleigh equation, equation (10), we obtain $(N-1)$ equations by equating the coefficients of the polynomials of degree n, $n = 2,..N$. The resulting system of equations can be expressed in the form of equation (7). The details of the application of the Chebyshev tau method to hydrodynamic stability problems can be found in Bridges and Morris[10] and Liou[16].

2.2 Chebyshev Collocation Method

It is well known that a smooth function, $F(z)$, can be approximated by polynomials in z. The resulting polynomials, such as the Lagrange interpolation polynomial based on equally spaced collocation points, however, typically diverge as the number of collocation points increases. The poor convergence behavior of polynomial interpolation can be avoided by relating the collocation points to the structure of orthogonal polynomials, like Chebyshev or Legendre polynomials. In the Chebyshev collocation (CC) method the collocation points, z_j are the extrema of the Nth order Chebyshev polynomials $T_N(z)$. That is,

$$z_j = \cos(\frac{j\pi}{N}), \qquad j = 0, \ldots, N \tag{12}$$

There are other choices of the collocation points[17]. The approximated solution becomes

$$\mathbf{v}(z) = \sum_{j=0}^{N} v(z_j)\, b_j(z) \tag{13}$$

where $b_j(z)$ are the expansion orthogonal functions. The approximation simultaneously interpolates the solution at each collocation point. That is,

$$b_j(z_i) = \delta_{ij} \tag{14}$$

The details of these expressions can be found in Voigt[17]. The resulting system of equations obtained by evaluating the differential equation, equation (5), at the collocation points can be put into the form of equation (7).

2.3 Finite Difference Method

The Rayleigh equation can also be discretized by finite difference (FD) methods The discretization is performed in the transformed plane where $z \in$ [-1,1]. The finite difference approximation to the Rayleigh equation at grid point i is

$$[-U_i\, \hat{v}_i]\alpha^3 + [\omega\hat{v}_i]\alpha^2 + [f_1(\frac{\hat{v}_{i+1} - \hat{v}_{i-1}}{2\Delta z}) + f_2(\frac{\hat{v}_{i+1} - 2\hat{v}_i + \hat{v}_{i-1}}{\Delta z^2}) + f_3\hat{v}_i]\alpha$$

$$+ [f_4(\frac{\hat{v}_{i+1} - \hat{v}_{i-1}}{2\Delta z}) + f_5(\frac{\hat{v}_{i+1} - 2\hat{v}_i + \hat{v}_{i-1}}{\Delta z^2})] = 0 \tag{15}$$

where

$$f_1 = (U\ m\ m')_i\ , \quad f_2 = (Um^2)_i\ , \quad f_3 = (-\omega m\ m')_i,$$

$$f_4 = (-\omega m^2)_i\ , \quad f_5 = (-m\ (mU')')_i. \qquad (i = 1 \ldots N)$$

$$\Delta z = \frac{2}{N-1}.$$

and N denotes the total number of the grid points. The first and the second derivatives are approximated by corresponding second order finite difference formulas. It is important to note that there are no additional computational difficulties if higher order difference formulas are used. The finite difference discretization has been found to be more straight forward to formulate than either the Chebyshev tau or the Chebyshev collocation methods described above. The application of the equation (15) at each grid point gives rise to a system of equations in the form of equation (7).

In the Chebyshev tau method, the eigenvectors of the eigenvalue problem give the spectrum of the expansion. While in the collocation and the finite difference method, the eigenvectors are the solution vectors themselves.

2.4 Boundary Conditions

The boundary conditions for the present problem are

$$\hat{v}(\pm\infty) = 0 \tag{16}$$

since the spatial instability waves must decay far from the shear layer. In the Chebyshev tau method, the boundary conditions become

$$\mathbf{v}(\pm 1) = \frac{v_0}{2} + \sum_{n=1}^{N} (\pm 1)^n v_n = 0 \tag{17}$$

The addition of these two equations to the set of equations formed in the approximations above closes the resulting system of equations. The coefficient matrices, when written in the form of equation (7), are of order $(N+1) \times (N+1)$. The homogeneity of the boundary conditions, however, allows us to reduce the order of the lamda matrix by column operations to $(N-1) \times (N-1)$. The form of the boundary conditions are the same for both the collocation and the finite difference methods. They are given by

$$\mathbf{v}(\pm 1) = 0 \tag{18}$$

The appropriate column operations and substitutions can once again reduce the order of the coefficient matrices to $(N-1) \times (N-1)$.

2.5 Eigenvalue and Eigenfunction Calculations

Two methods are used to solve the eigenvalue problem, equation (7), in which the parameter is of order three. The LCM linearizes the problem and reduces it to a general eigenvalue problem. But the resulting companion matrix for the matrix polynomial is of higher order, $3 \times (N-1)$, in the present case. The method, nevertheless, provides an approximation to the complete eigenvalue spectrum. The matrix factorization method features only a subset of the eigenvalue spectrum. The method, however, involves only matrices of order $(N-1)$. The details of these two methods can be found in Bridges and Morris[10].

In general, the continuous part of the eigenvalue spectrum may be ignored when seeking only criterion for stability[18]. In order to numerically distinguish the discrete part from the continuous part of the spectrum, a transformation is used in conjunction with the matrix factorization method. The transformation is

$$\hat{\alpha} = \frac{1}{(\alpha_f - \alpha)} \tag{19}$$

The lambda matrix then becomes

$$\hat{D}_3(\hat{\alpha}) \;=\; \hat{\mathbf{C}}_0\hat{\alpha}^3 \;+\; \hat{\mathbf{C}}_1\hat{\alpha}^2 \;+\; \hat{\mathbf{C}}_2\hat{\alpha} \;+\; \hat{\mathbf{C}}_3 \tag{20}$$

This transformation would insure that the eigenvalues of $D_3(\alpha)$ in the vincinity of α_f appear in the set of eigenvalues of the dominant solvent of $\hat{D}_3(\hat{\alpha})$. A solvent of $\hat{D}_3(\hat{\alpha})$ is said to be dominant if every eigenvalue in the set has an absolute value greater than all the eigenvalues of $\hat{D}_3(\hat{\alpha})$ that are not in it. An algorithm developed by Dennis et al.[19] has been used to find the dominant solvent of the matrix polynomial. The desired eigenvalue can then be identified. The eigenvalues obtained from each of the previous methods may be further refined by the iterative method of Lancaster[20]. To compute single eigenvectors the inverse iteration method is used,

$$\mathbf{D}(\alpha_k)\ \mathbf{v}^{k+1} \;=\; \varrho\mathbf{v}^k \tag{21}$$

where ϱ is a scaling factor and is taken as 1 in the calculation. The initial guess for the iteration is the complex unit vector.

In this section, we have summarized three global approaches to solve the eigenvalue problem generated by the spatial stability analysis of a free shear layer, in which the eigenvalue appears in a nonlinear manner. The eigenvalues will be calculated using both the LCM and the matrix factorization methods. The results of our computations are presented in the next section.

3. RESULTS AND DISCUSSION

In this section, a comprehensive comparison of the different numerical methods is presented in terms of their accuracy and efficiency in solving the spatial, inviscid instability of a free mixing layer.

The velocity profile for the basic free shear layer is chosen to be

$$U(y) = \frac{1}{2}(1 + \tanh(y)) \tag{22}$$

The physical domain is transformed to the domain [-1,1] on which Chebyshev polynomials are defined. Grosch and Orszag[21] studied spectral solutions of differential equations in both semi-infinite and infinite domains and used three types of transformations. These included a domain truncation, an algebraic mapping and an exponential mapping. They found that all of the three transformations are useful if the exact solution of the original differential equation decays exponentially fast as $| y | \rightarrow \infty$, but fail if solutions oscillate out to infinity. Their results also showed that when the solution of a problem is smooth in the mapped domain algebraic mappings are preferred over the other two. Since the solution of the Rayleigh equation in the regions of constant mean flow properties can be written as,

$$\hat{v} \approx \exp\left[\mp\alpha y\right] \quad \text{as} \quad y \rightarrow \pm\infty \tag{23}$$

a square-root transformation is used in the present analysis to avoid the singularities at the end points of the transformed domain, $z = \pm 1$, which would arise if an exponential mapping was used[21]. As will be seen later, the square-root transformation also enables the CC and the FD methods to predict accurately the continuous spectrum associated with the unboundedness even though the corresponding eigensolutions are highly oscillatory at infinity. The transformation used is,

$$z = \frac{y}{(r^2 + y^2)^{1/2}} \tag{24}$$

where r is a scaling factor. The metric dz/dy is

$$m = \frac{(1 - z^2)^{3/2}}{r} \tag{25}$$

The scaling factor r controls the distribution of grid points. Increasing r decreases the number of grid points clustered around $y = 0$. Since the scaling factor determines the amount of the domain stretching, its optimum value, for which the solutions are most accurate, may depends on both the number of grid points used and the discretization scheme. However, the best grid distribution should be the same for a given problem, irrespective of the discretization scheme. Boyd[22] used a steepest descent method to predict the optimum choice of the mapping parameter in applying a Chebyshev polynomial approximation to a known, explicit function. Nevertheless, computing analytically the optimum mapping parameter in the application of global approximations to a differential equation is difficult. Some preliminary numerical tests were performed using the matrix factorization method to evaluate the effects of domain stretchings on the prediction of the discrete eigenvalue spectrum . For $\omega = 0.2$ and $N = 17$, the results are given in Table 1. The error, ϵ, in each case is based upon the corresponding solutions from a shooting method and is determined by

$$\epsilon = \left|\frac{\alpha - \alpha_s}{\alpha_s}\right| \tag{26}$$

where α_s is the eigenvalue calculated by the shooting method. This yields the value

$$\alpha_s = 0.38260 - i0.22762. \tag{27}$$

In the shooting method the Rayleigh equation was integrated in the interval $y \in [-6, 6]$ in 200 steps using a fourth-order, fixed step size Runge-Kutta procedure. Note that the solution decays exponentially at the far field and the center region around $y = 0$ is the region where there are large changes of the solution. To start a calculation, therefore, one can set $r = 1$. Since

$$m\ (z = 0) = 1.0 \tag{28}$$

the region around $z = 0$, where there are large changes of flow properties, is not scaled for $r = 1$. Table 1 shows that the best scaling factors for the FD, the CC and the CT methods are 2.5, 2.0 and 2.5, respectively. Since the finite differencing is performed on equally spaced grids and the collocation points in the collocation method cluster at both ends of the computational domain, more domain stretching, or a bigger r, is needed for the finite differencing than for the collocation method. With $N = 17$, however, the dependence on the stretching parameters seems rather weak. The eigenvalues predicted by all the discretization methods are within 1% of the value obtained by using the shooting method. As will be shown later, this weak dependence quickly disappears as N increases. In the following calculations, the scaling factors used are the "optimum values" for each case unless otherwise noted.

Tables 2 and 3 give the order of the coefficient matrices required by each method to obtain 10% and 1% of accuracy in the eigenvalue calculations, respectively.

Table 1 Predicted Eigenvalues. $\omega = 0.2$, $N = 17$.

r	F D	ϵ	C C	ϵ	C T	ϵ
0.5	(0.38053,-0.14657)	0.18	(0.41107,-0.24395)	0.073	(0.36949,-0.18014)	0.11
1.0	(0.35426,-0.22327)	0.064	(0.38119,-0.22371)	0.009	(0.37514,-0.23469)	0.023
1.5	(0.37896,-0.23947)	0.028	(0.38171,-0.22870)	0.003	(0.38455,-0.22343)	0.006
2.0	(0.38575,-0.22985)	0.009	(0.38290,-0.22834)	0.002	(0.38304,-0.22756)	0.001
2.5	(0.38423,-0.22496)	0.007	(0.38313,-0.22931)	0.004	(0.38265,-0.22819)	0.001
3.0	(0.38231,-0.22319)	0.01	(0.38559,-0.23188)	0.012	(0.38319,-0.22877)	0.003
4.0	(0.38114,-0.22187)	0.013	(0.37169,-0.20992)	0.047	(0.38615,-0.23072)	0.011
5.0	(0.38299,-0.22050)	0.016	(0.34586,-0.23982)	0.087	(0.38964,-0.23328)	0.034

It can be seen that the FD discretization predict the discete eigenvalue to the same order of accuracy as the CT and the CC methods do with the lowest order of the coefficient matrices. The two spectral methods performed almost equally well with proper choices of the mapping parameters. All the three discretization methods show rapid convergence at the low values of N.

Table 2 Predicted Eigenvalues of less than 10% error. $\omega = 0.2$.

	N	r	α_r	$-\alpha_i$	$\epsilon \times 10^2$
FD	5	2.0	0.38334	0.19239	7.9
CC	8	1.5	0.38870	0.21940	2.2
CT	7	2.5	0.41960	0.20607	9.6

Table 3 Predicted Eigenvalues of less than 1% error. $\omega = 0.2$.

	N	r	α_r	$-\alpha_i$	$\epsilon \times 10^2$
FD	9	2.5	0.38364	0.22812	0.3
CC	11	1.5	0.38264	0.22364	0.9
CT	10	3.0	0.38498	0.22597	0.6

For the CC and the CT methods, the calculated eigenvalues converge from 10% to 1% error by increasing the number of the approximation functions by about 30%. The reason is that in the mapped domain equation (23) becomes

$$\hat{v} \approx \exp\left[\mp \frac{\alpha r z}{(1-z^2)^{1/2}} \right] \text{ as } z \to \pm 1 \tag{29}$$

The solution is thus smooth in the mapped domain and the rapid convergence property of the global methods is retained. Comparisons of the rates of convergence for the various discretizations and solution techniques are given for the case $\omega = 0.2$ in Table 4. All of the discretization methods show rapid (faster than algebraic) rates of convergence when the LCM is applied. Similarly, the MF method also gives the same rapid rate of convergence using the CT and the CC methods. As was expected, the finite difference discretization predicts the eigenvalues well but with lower rates of convergence.

Note that the maximum computer time required in all the calculations in Table 4 is less than a minute on a VAX 8550 machine. In practical applications, therefore, the effect of the mapping parameter can be effectively minimized by increasing the order of approximations, or N, without a significant increase in computer time. This is also evident in the following eigenfunction calculations. Figures 1 and 2

Table 4. Errors ($\epsilon \times 10^2$) of the predicted eigenvalues.

	r	N					
		10		20		28	
		MF	LCM	MF	LCM	MF	LCM
F D	2.5	1.28	1.29	0.58	0.06	0.32	0.04
C C	2.0	3.01	1.29	0.08	0.08	0.02	0.02
C T	2.0	3.03	0.03	0.12	0.12	0.03	0.03

(a)

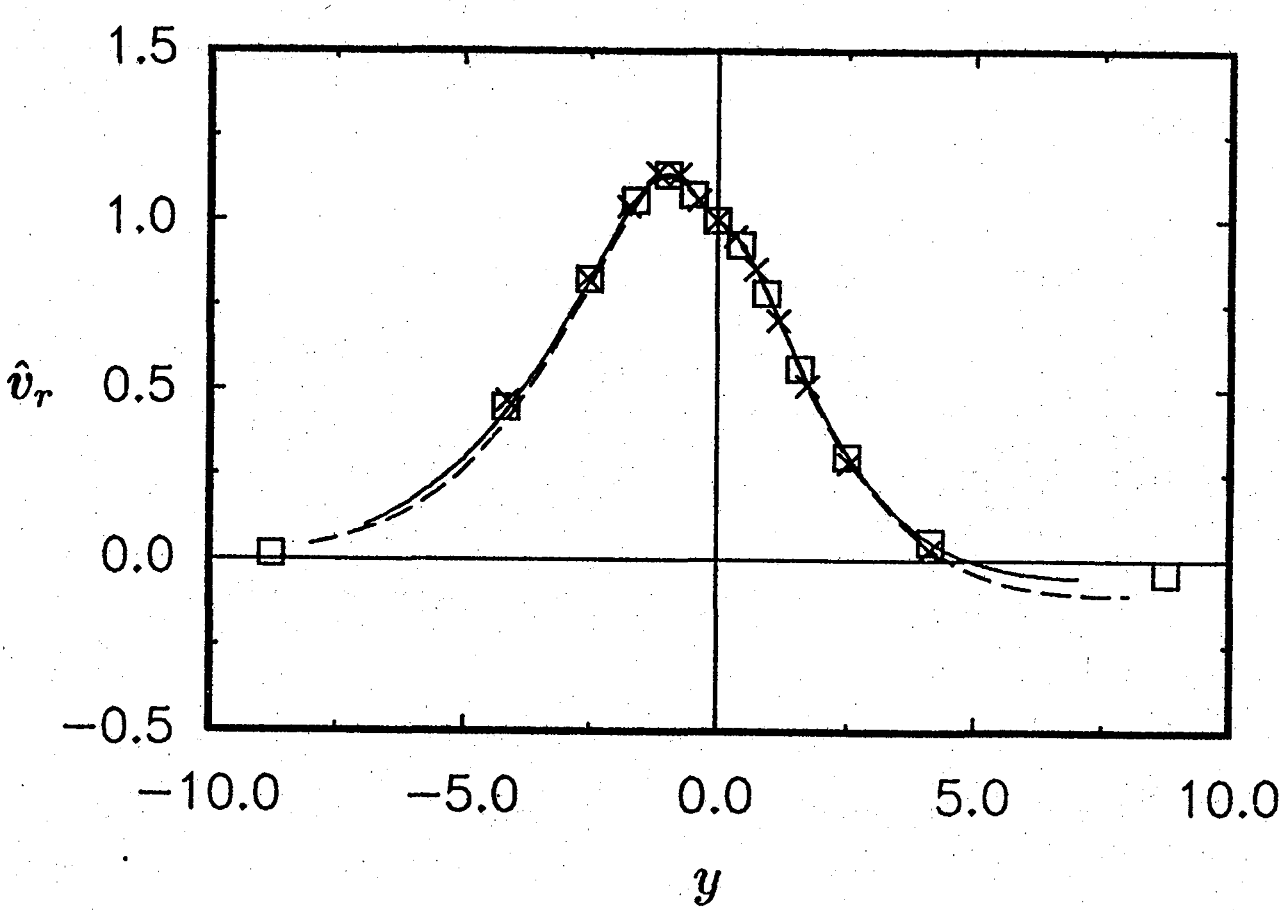

Figure 1. Eigenfunction for $\omega = 0.2$, $N = 13$ using ——— , Shooting Method; — — , CT; ▫ , CC; × , FD. (a) Real Part, (b) Imaginary Part.

(b)

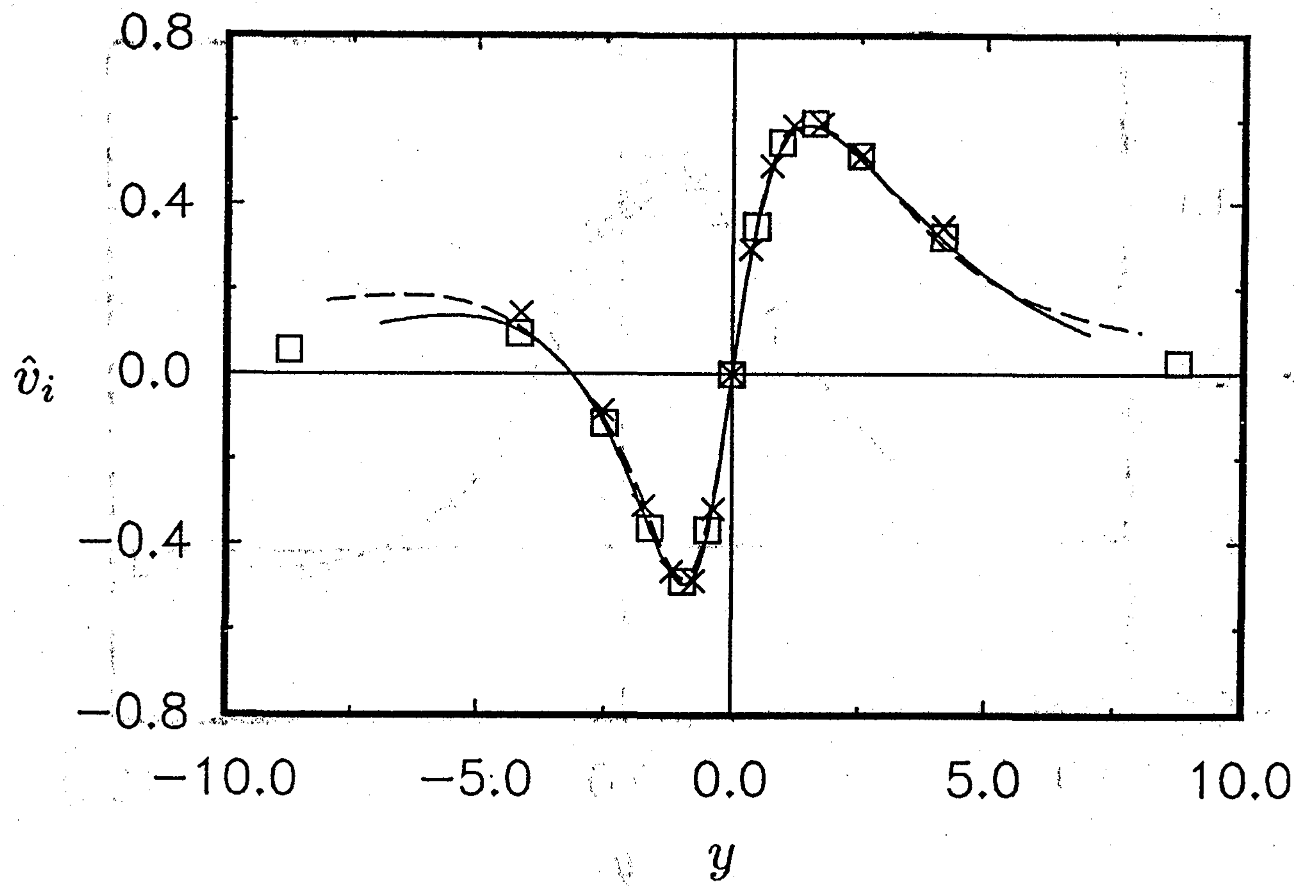

Figure 1. (continued)

(a)

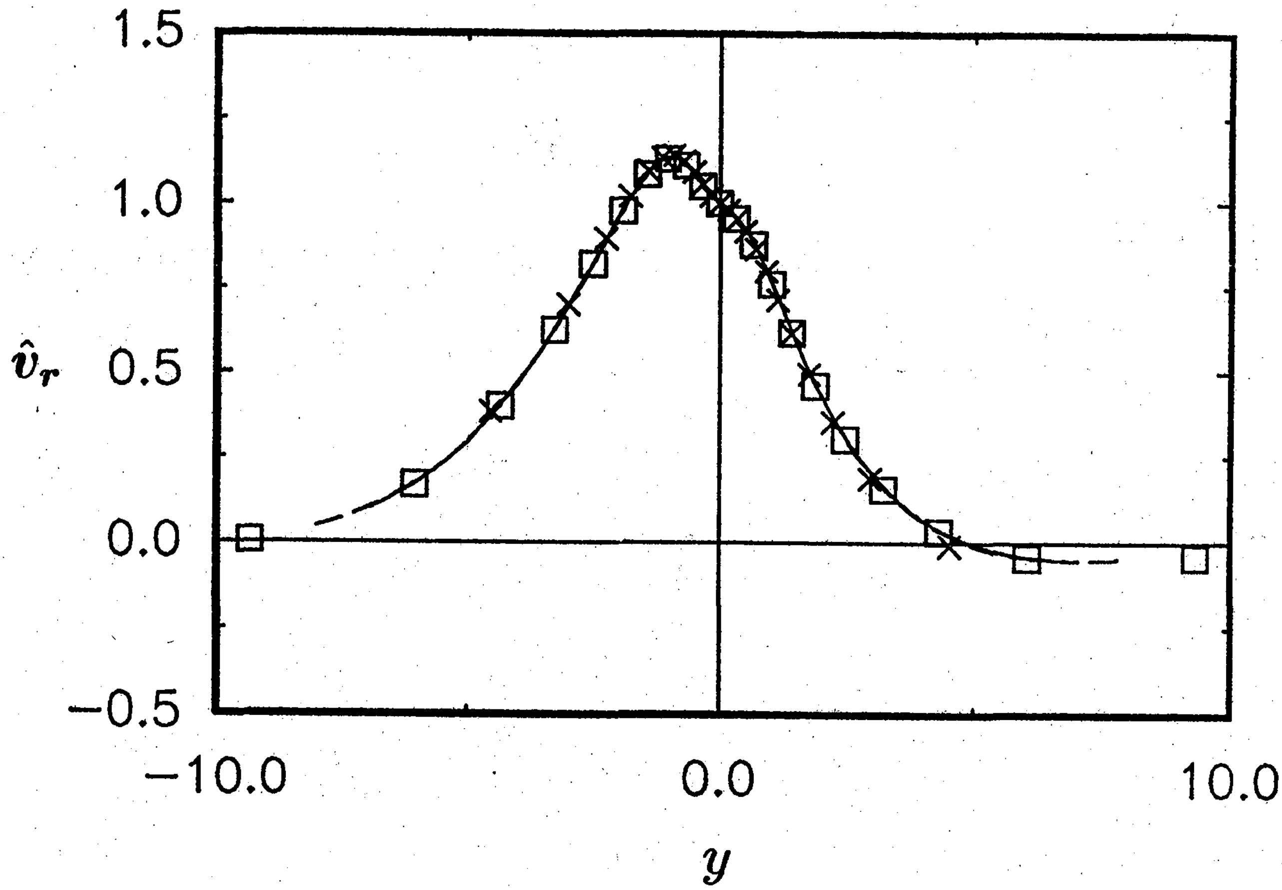

Figure 2. Eigenfunction for $\omega = 0.2$, $N = 23$ using ——— , Shooting Method; — — , CT; ◻ , CC; × , FD. (a) Real Part, (b) Imaginary Part

(b)

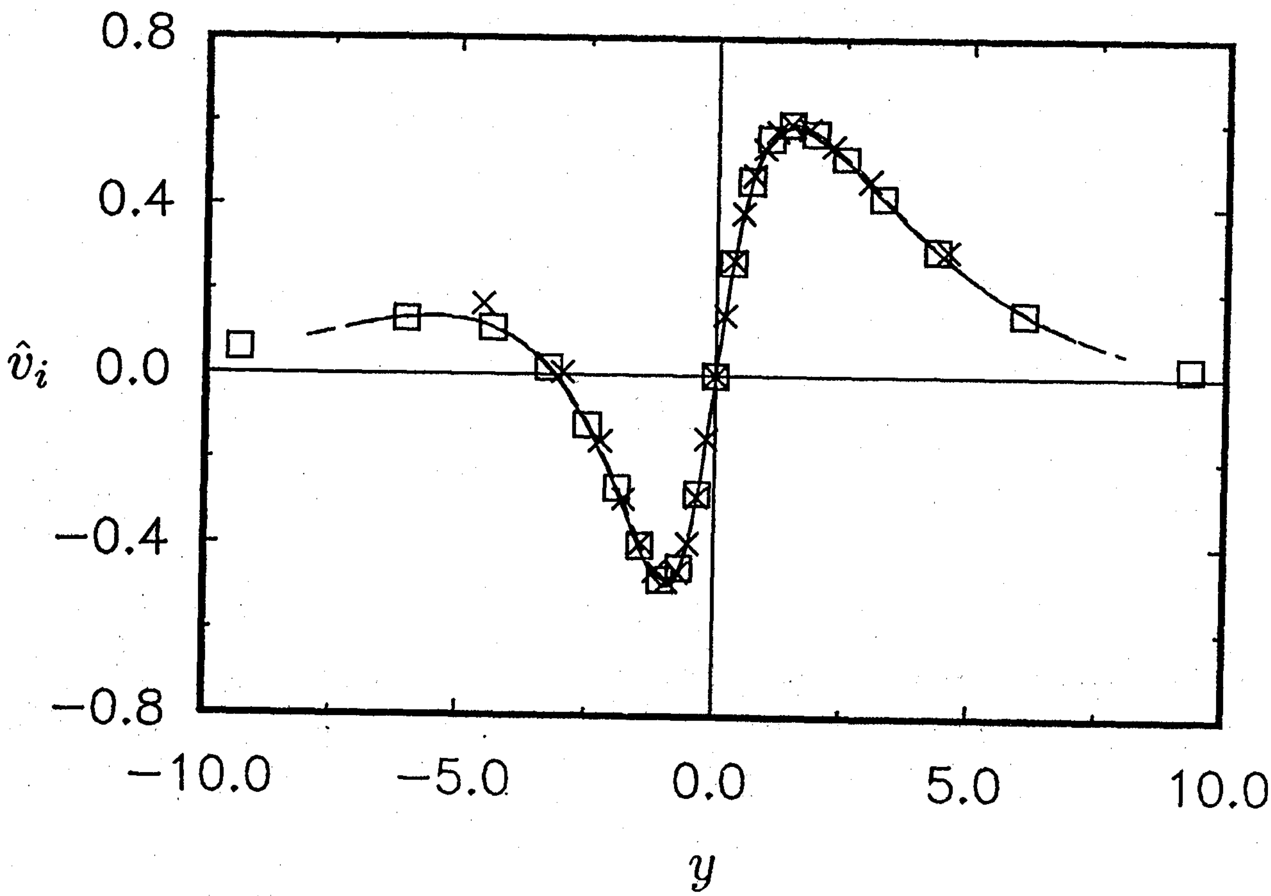

Figure 2. (continued)

show the real and the imaginary parts of the calculated eigenfunctions for cases with $\omega = 0.2$ and N=13 and 23, respectively. The error, ϵ, of the corresponding calculated eigenvalues was less than 1%. The agreement between the results is excellent even in the cases with N=13. For the discrete mode, all the methods become less sensitive to the choice of the scaling factors as N increases. While the spectral methods performed better than the finite difference method in other calculations[6,23], the finite difference formulation is competitive in the present application. Thus, the choice of solution methods appears to be problem-dependent.

As can be seen from Table 5, the eigenvalues calculated by using the LCM argee to the fourth digits with those from the MF method for all the discretization methods.

Table 5 Predicted Eigenvalues. $\omega = 0.2, N = 17$.

	LCM	MF	r	$\epsilon \times 10^2$
FD	(0.38421,-0.22494)	(0.38423,-0.22496)	2.5	0.7
CC	(0.38289,-0.22834)	(0.38290,-0.22834)	2.0	0.2
CT	(0.38304,-0.22755)	(0.38304,-0.22756)	2.0	0.1

The α_f in the matrix factorization method are chosen such that

$$\alpha_f = \alpha_s. \tag{30}$$

and the eigenvalues thus obtained are not refined by iterative methods. The α_s, however, are not always known *a priori* for other flow conditions. For example, the realistic velocity profiles of mixing layers may be different from the one assumed here and, therefore, their eigenvalues may be different. It may thus be difficult to obtain converged eigensolutions using the shooting method. The eigenvalues and the corresponding ϵ for other choices of α_f are shown in Table 6. Both the FD and the CT methods give good results for up to 30% under-shoot of α_f, for which the shooting method would have failed had the α_f been used as an initial guess. Therefore, in conjunction with the FD and the CT methods, the MF method is far less sensitive to the choice of α_f than the shooting method is to its initial guess. On the other hand, the Chebyshev collocation discretization is more sensitive to the α_f.

Figure 3 shows the growth rates of the spatially unstable modes of the free shear layer obtained by the various methods for $N = 11$. It was found that since the eigenfunctions decay more slowly in the far field as the frequency decreases, the mapping parameters selected for the mid frequency waves were not appropriate for the high and the low frequency wave calculations. The stretching parameters used were thus greater in the low frequency cases and smaller for the high frequencies. As was discussed earlier, the dependence quickly diminishes as N increases.

Table 6. Eigenvalues and errors ($\epsilon \times 10^2$) predicted using the matrix factorization method.

	α	$\epsilon \times 10^2$
$\alpha_f = (-0.3, 0.2)$,	$\left\lvert\frac{\alpha_f - \alpha_s}{\alpha_s}\right\rvert \times 10^2 = 20.0$	
F D	(0.376827,-0.224554)	1.4
C C	(0.283691,-0.203911)	22.0
C T	(0.377169,-0.220236)	2.1
$\alpha_f = (-0.228, 0.132)$,	$\left\lvert\frac{\alpha_f - \alpha_s}{\alpha_s}\right\rvert \times 10^2 = 30.0$	
F D	(0.373056,-0.214566)	3.6
C C	(0.232942,-0.263733)	34.5
C T	(0.374547,-0.204189)	5.5

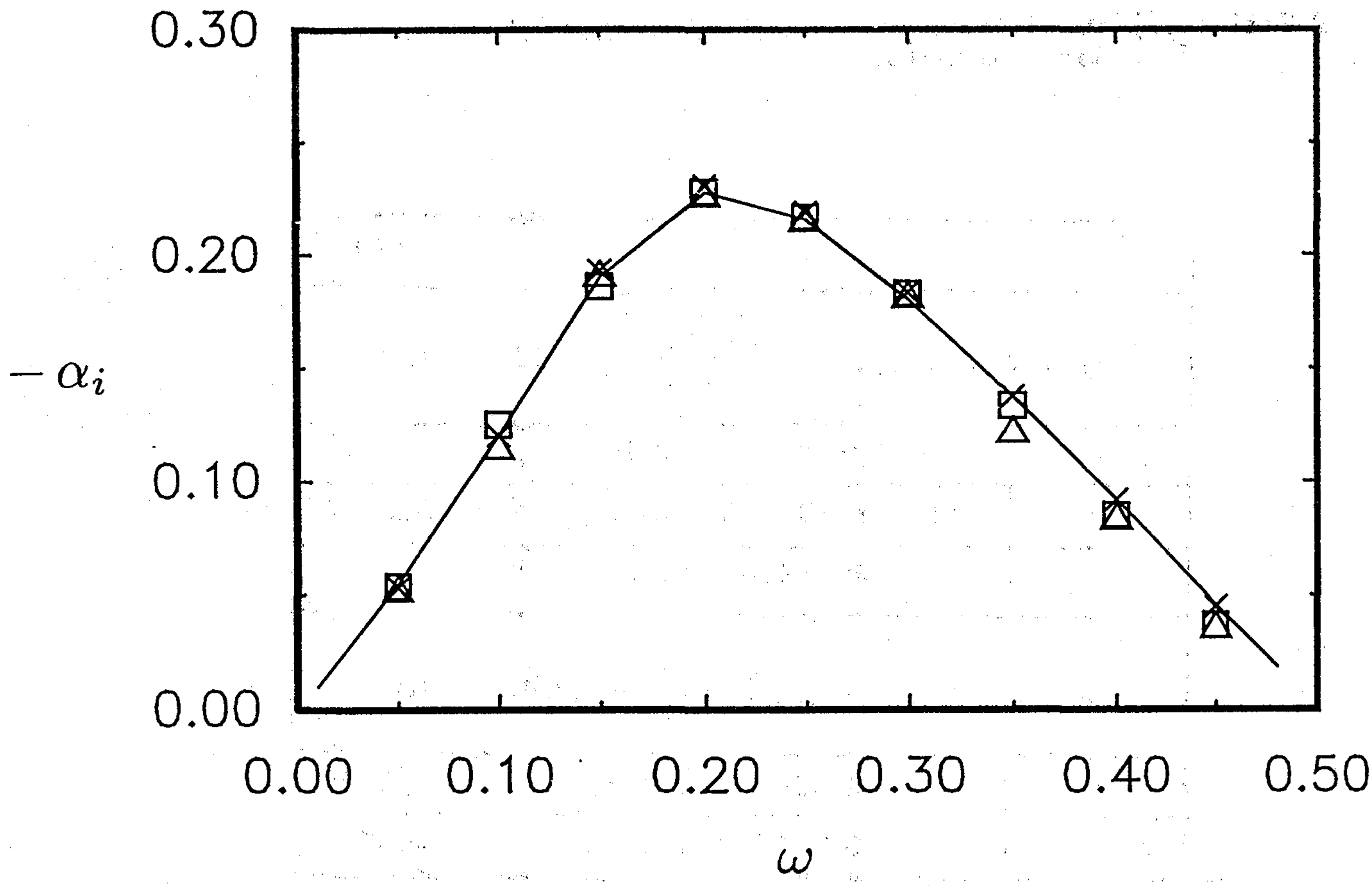

Figure 3. Spatial Growth Rates ($-\alpha_i$). ——— , Shooting Method; △ , CT; □ , CC; × FD.

One of the advantages of using the global approaches is that we obtain an approximation to the complete eigenvalue spectrum, while in the shooting method each eigenvalue has to be determined separately. In addition to a finite number of discrete values of α that satisfies the dispersion relation (3), there are also continuous branches associated with the singularity of the Rayleigh equation. In the present stability calculations, for example, there are two continuous branches of the eigenvalue spectrum arising from the singularity, y_c, of the Rayleigh equation, where

$$\alpha \; U(y_c) \; - \; \omega \; = \; 0. \tag{31}$$

For the hyperbolic-tangent velocity profile assumed here, these singular spectra are

$$\text{(i)} \qquad \alpha_i \; = \; 0 \; ; \; \alpha_r \; \geq \omega \tag{32}$$

$$\text{(ii)} \qquad \alpha_i \; \in \; \mathrm{R} \; ; \; \alpha_r \; \rightarrow \; \infty. \tag{33}$$

Figure 4a shows the calculated results with N=17 and ω=0.2 using the FD and the LCM methods. The spectrum associated with the equations (32) can be clearly seen; however, the one associated with the equation (33) is cut out due to the magnitude of eigenvalues.

Another continuous spectrum that can be observed in Figure 4 is associated with the bounded solutions of the asymptotic form of the Rayleigh equation in the far field,

$$\hat{v}'' \; - \; \alpha^2 \; \hat{v} \; = \; 0. \tag{34}$$

since $U'' \; \rightarrow \; 0$ as $y \; \rightarrow \; \pm\infty$. This is the continuous spectrum associated with the domain unboundedness and can be written as

$$\alpha_r \; = \; 0, \qquad \alpha_i \; \in \; \mathrm{R} \tag{35}$$

The corresponding eigenfunctions are purely perodic. As is shown in Figure 4b the numerical results predict better both of the continuous spectra, equation (32) and (35), with larger values of N. The finite approximations used here will converge to the solution of the equation as $N \rightarrow \infty$. Similar characteristics of the eigenvalue spectrum have been observed in plane Couette flow calculations[16]. The discrete part of the spectrum is associated with the convective instability. For ω=0.2, the plane Couette flow is stable and the discrete spectrum is empty. Case[24] obtained eigenfunctions corresponding to the eigenvalues in these singular branches by taking a Fourier transform with respect to x and a Laplace transform with respect to time of the linearized disturbance equations. The resulting equation is then solvable using a Green's function method. The method is applicable to the current cases, but will not be given here.

(a)

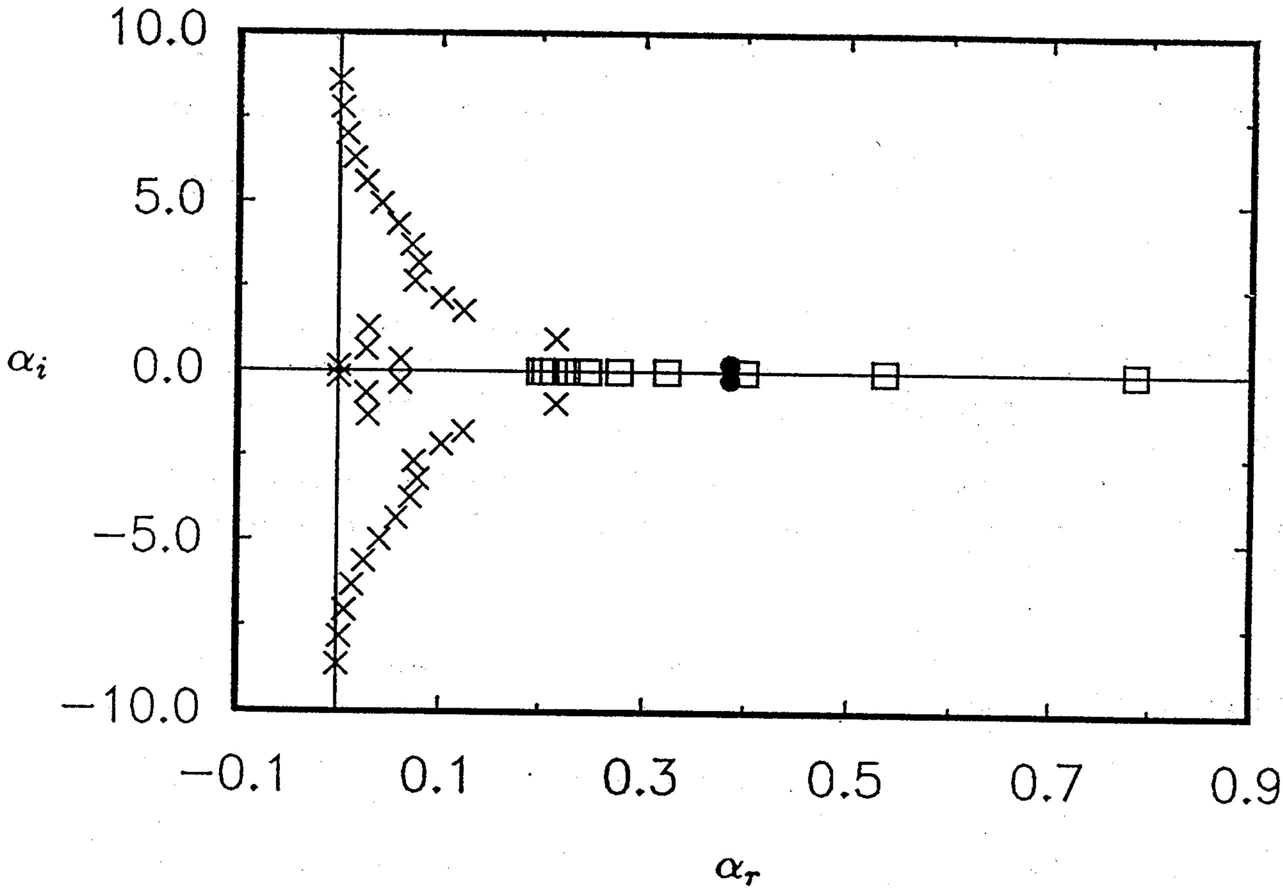

Figure 4. Eigenvalue Spectra. $\omega = 0.2$. × , Eigenvalues Associated with the Unbounded Domain; □ , Eigenvalues Associated with the Singularity of the Rayleigh Equation; • , Discrete Spectrum. (a) $N = 17$, (b) $N = 76$.

(b)

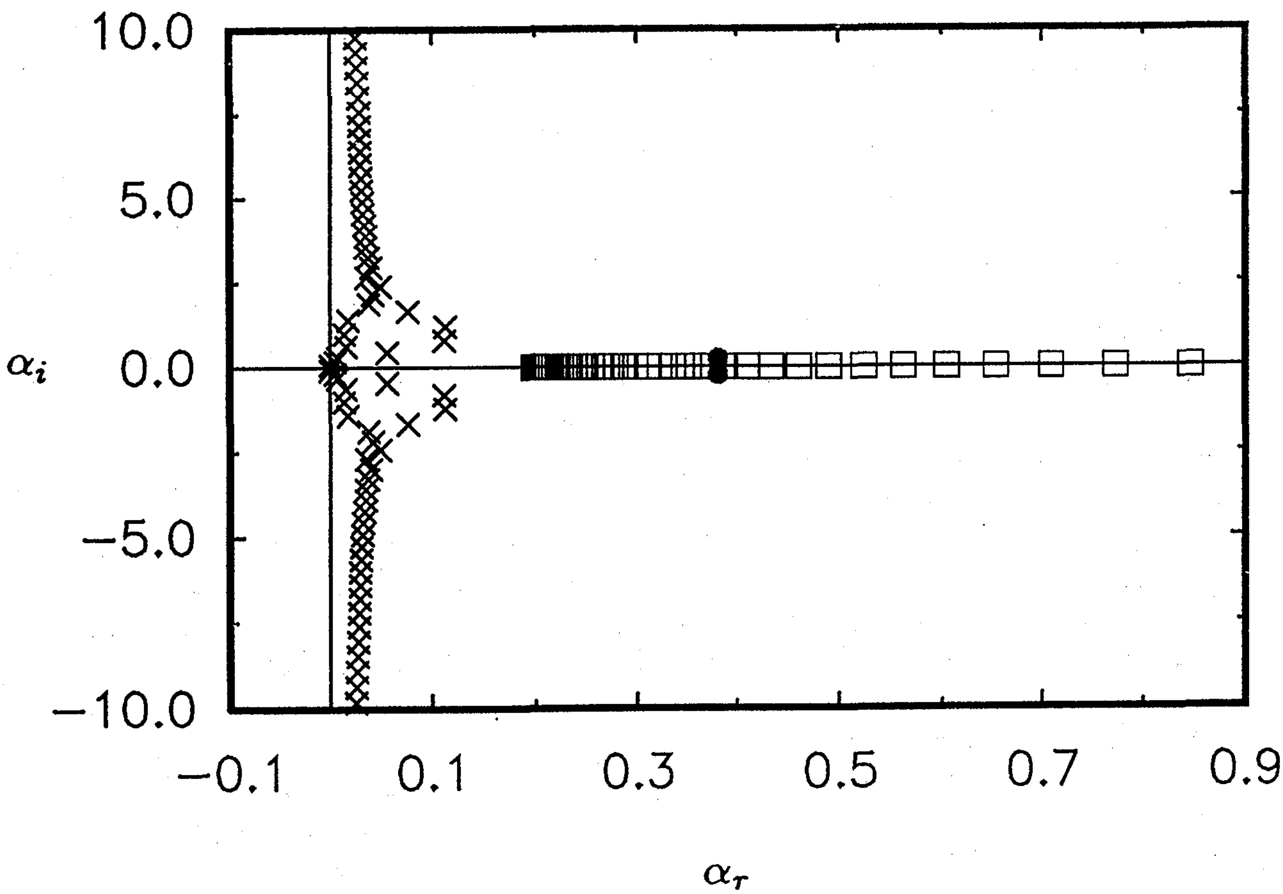

Figure 4. (continued)

Figure 4 also shows that the presence of these continuous eigenvalue spectra may conceal or mask the discrete eigenvalues. The spurious solutions, however, are far away from the discrete spectrum in the complex wave speed plane. Figure 5 shows this tendency clearly. The complex wave-speed of the discrete mode for ω=0.2 is (0.51845,-0.87404). Thus, the discrete spectrum can be better observed in the wave-speed plane.

If a transformation that produces singularities at the boundaries of the transformed domain is used, the convergence property of the global approximations would no longer be retained. Figure 6 shows the approximated eigenvalue spectrum using a hyperbolic-tangent transformation the CT method and the LCM method for $\omega = 0.2$ and $N = 27$. The transformation is

$$z = \tanh(y). \tag{36}$$

Both the discrete and the continuous spectra are not well predicted even with the relative high order of approximation.

Figures 7a, 7b and 7c show the eigenvalue spectrum with $\omega = 0.2$ using the CC, the FD and the CT methods, respectively, and the square-root transformation. The spectra associated with the equation singularity, equations (32) and (33) and the discrete spectra are well predicted. As was discussed earlier, the convective instability described by the discrete spectrum is associated with the local vorticity distribution and is less sensitive to r as N increases. It can be observed from the present results that the same is true for the continuum due to the equation singularity. Despite the oscillatory nature of the corresponding eigenfunctions as $y \to \infty$, the locations of the continuous spectra associated with the domain unboundedness predicted by the CC and the FD also agree well with the analytic expression, equation (35). The square-root transformation used here seems to be a viable alternative to the three transformations tested by Grosch and Orszag[21] for either the FD or the CC methods. However, the continuum predicted by the CT method is very sensitive to the mapping parameter, r, even for the relatively high values of N. This may be due to the aliasing terms that are not included in the Chebyshev spectral tau methods. The eigenvalue spectrum is made complete with the inclusion of the continuous branches and an arbitrary initial disturbance can not be represented without knowing the complete eigenvalue spectrum. Therefore, a good approximation of the eigenvalue spectrum associated with the domain unboundedness is important to the solution of the Rayleigh equation in an unbounded domain.

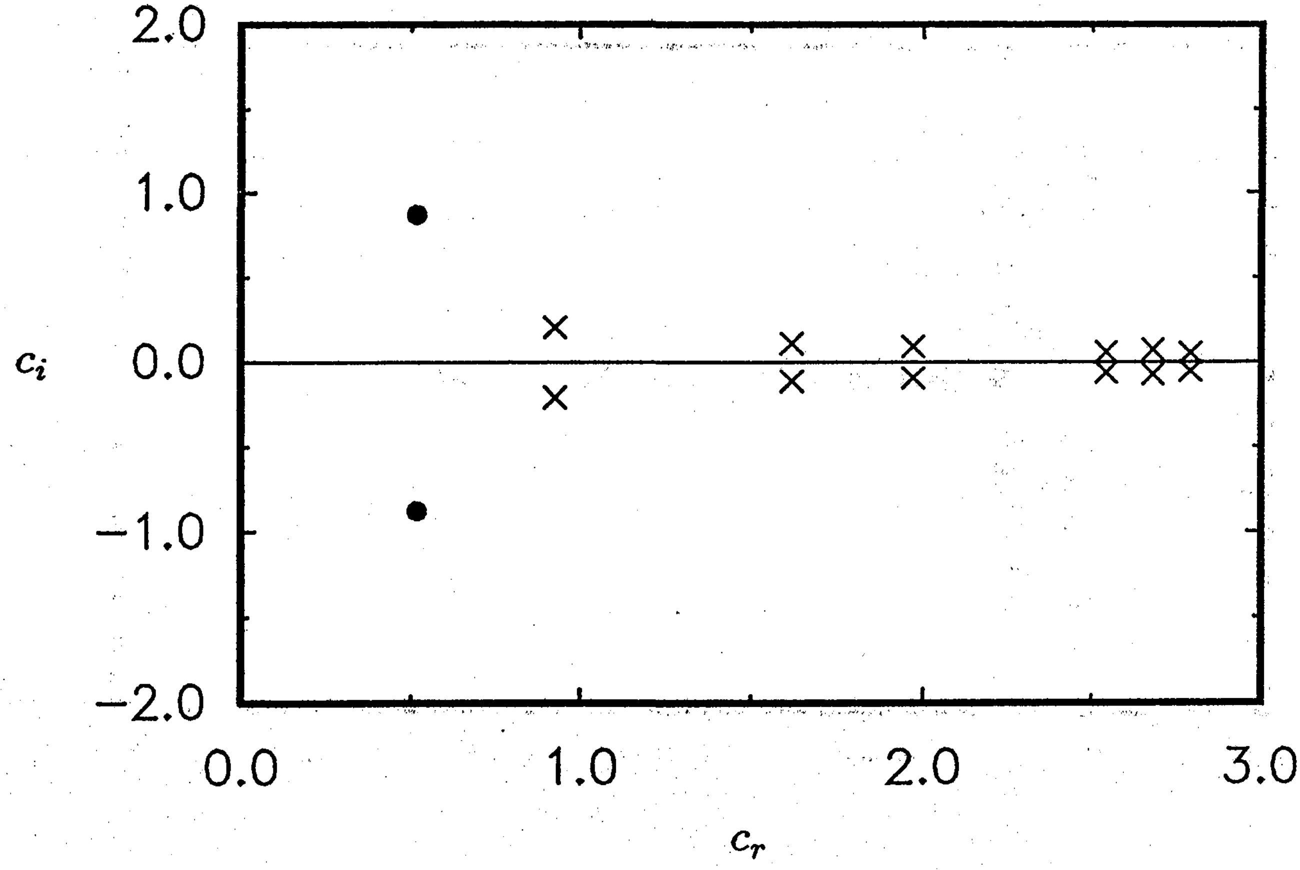

Figure 5. Complex Wave-Speed. $\omega = 0.2$, $N = 17$. Legend: See Figure 4.

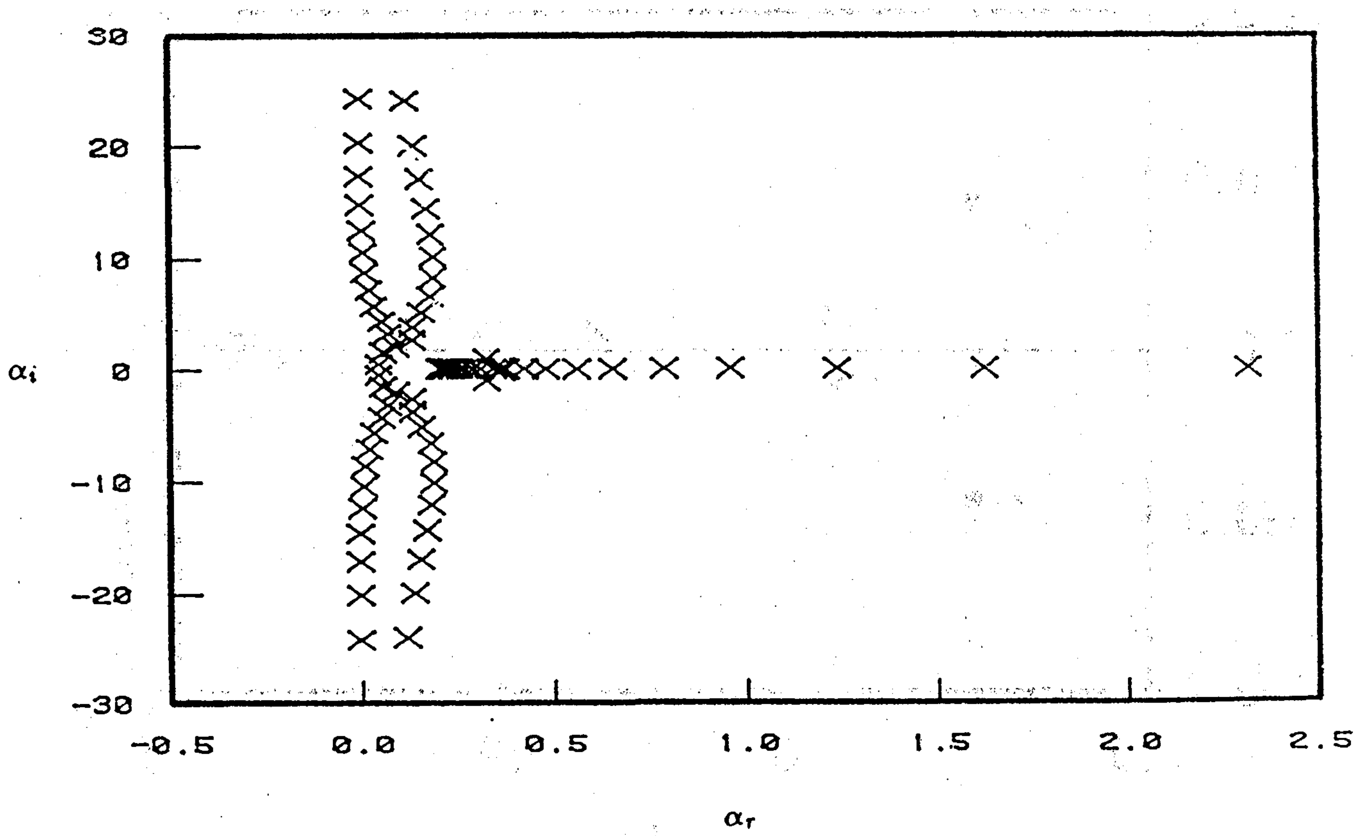

Figure 6. Eigenvalue Spectra with the Hyperbolic-Tangent Transformation. $\omega = 0.2$, $N = 27$. Source: Liou (1986)

(a)

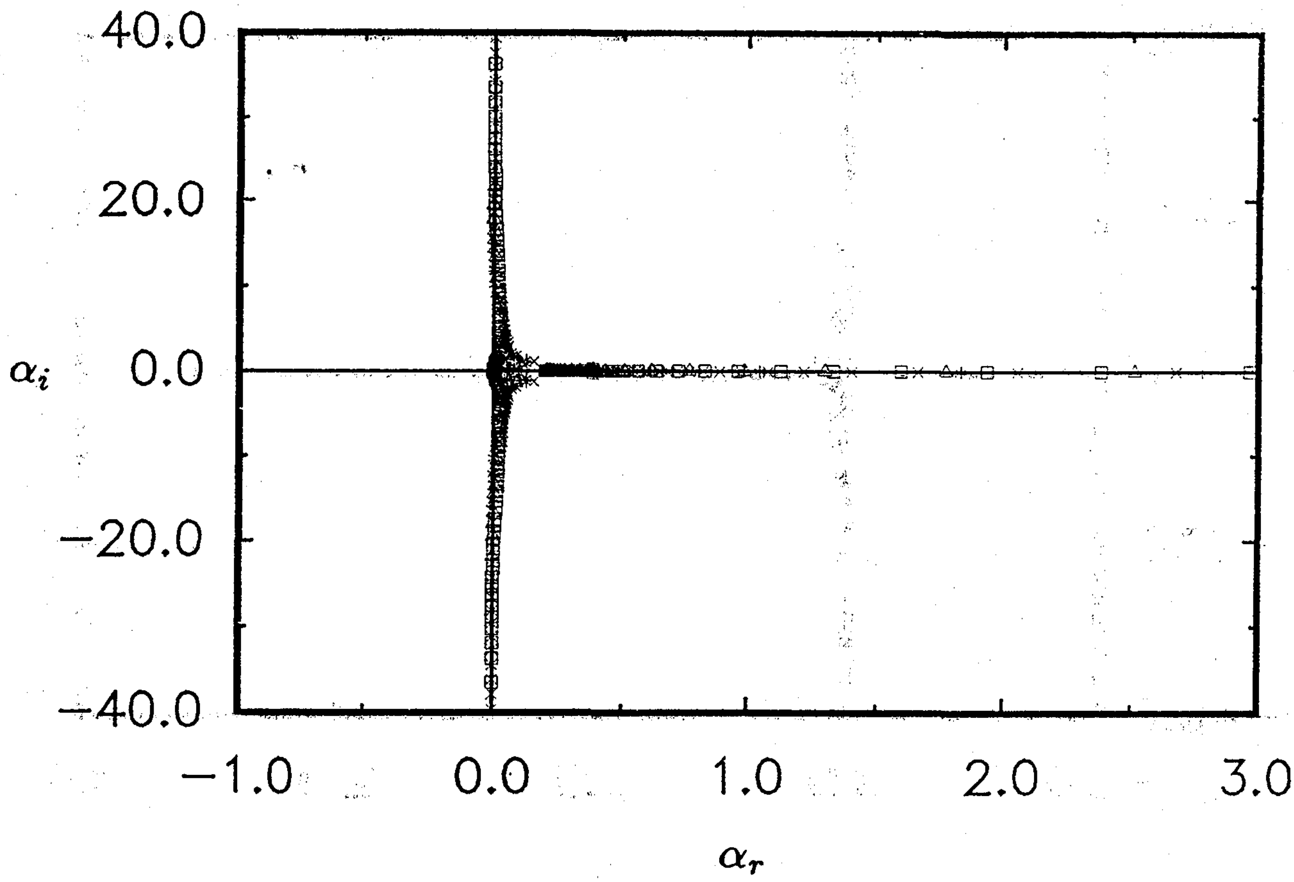

Figure 7. Eigenvalue Spectra for $\omega = 0.2$. $*$, $N = 26$, $r = 2.0$; $\triangle$, $N = 46$, $r = 2.0$; $\square$, $N = 76$, $r = 2.0$; $\times$, $N = 76$, $r = 0.5$. (a) Chebyshev Collocation Method , (b) Finite Difference Method, (c) Chebyshev Tau Method.

(b)

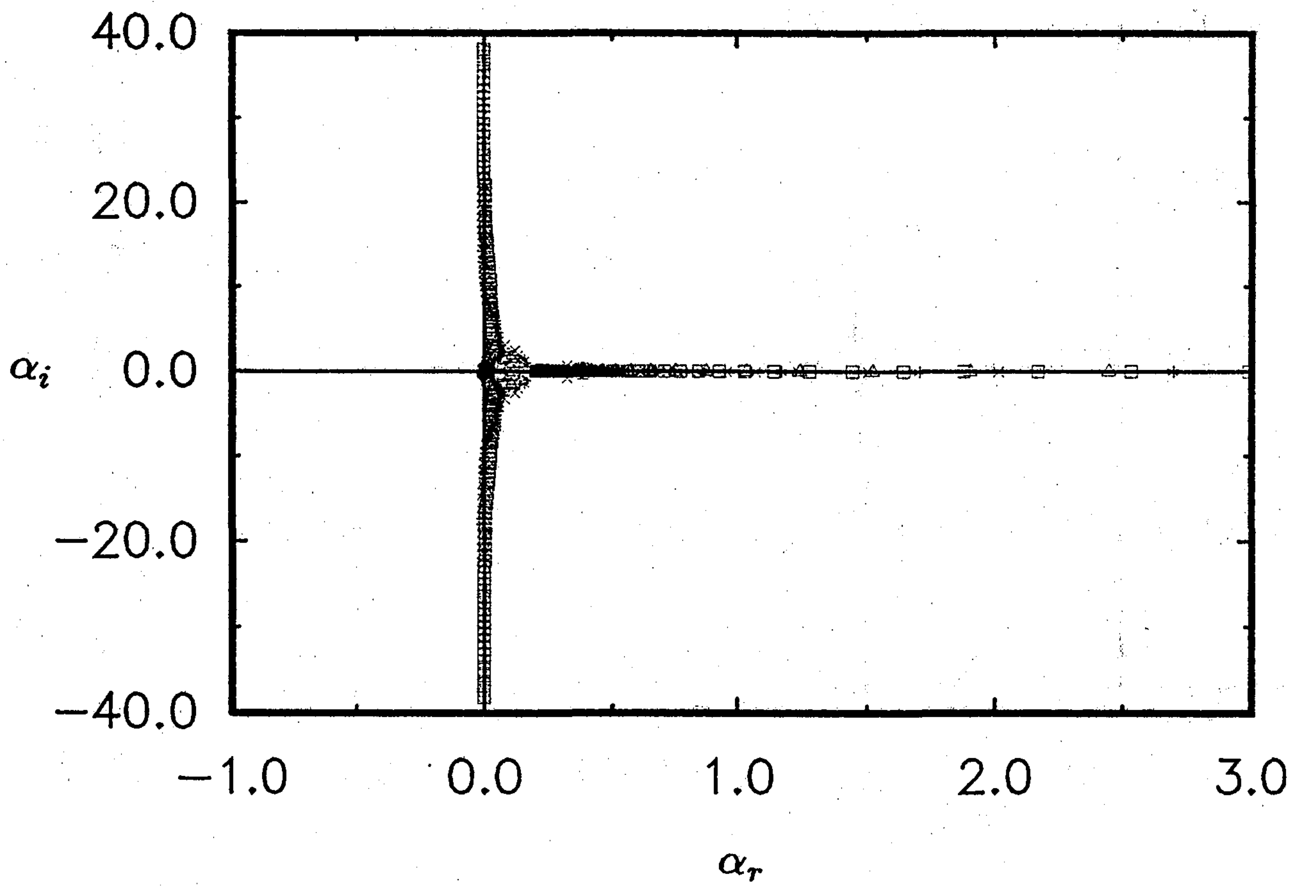

Figure 7. (continued)

(c)

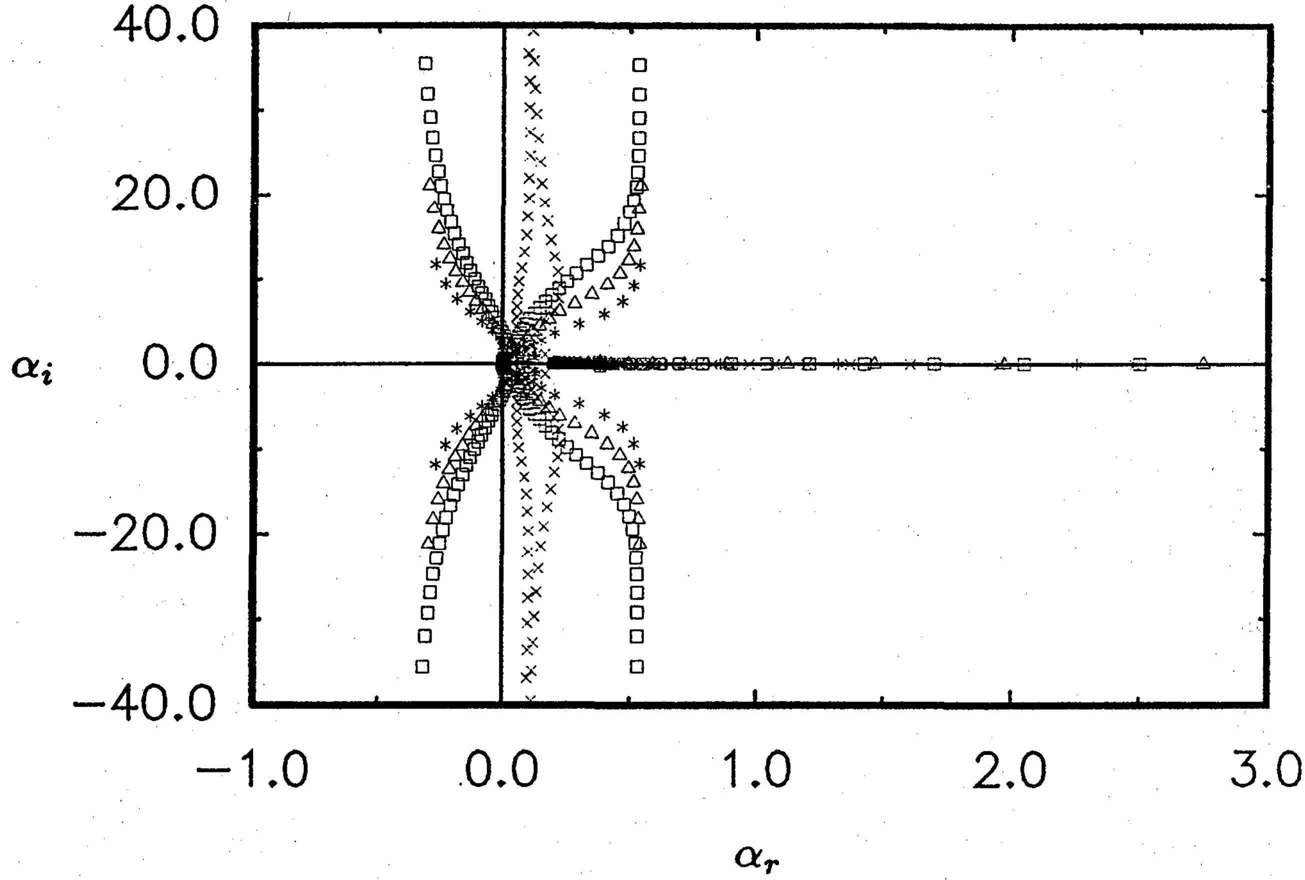

Figure 7. (continued)

4. CONCLUSIONS

Three discretization schemes, two spectral methods and a finite difference method have been applied to solve the spatial inviscid instability of a free mixing layer with a hyperbolic-tangent velocity profile. Calculated eigenfunctions for the discrete mode using these global approximations show good agreement with that using a conventional shooting procedure. For the same order of accuracy of the calculated eigenvalues, when compared to that using the shooting method, the finite difference discretization is more efficient than both the Chebyshev tau and the Chebyshev collocation methods. On the other hand, the Chebyshev tau method is more efficient than the Chebyshev collocation method. The finite difference method is also easier to formulate and code. All of the three discretization schemes result in rapid rates of convergence when the LCM is used. The matrix factorization is less sensitive to the α_f than the shooting method is to its initial guess. The α_f appears in the transformation that was used to identify the discrete eigenvalue. The LCM is preferred when the eigenvalue desired is not known *a priori*. The discrete part of the eigenvalue spectrum is very distinguishable in the complex wave speed plane.

All of the discretization methods used here, the second-order finite difference, the Chebyshev tau and the Chebyshev collocation methods, are capable of predicting accurately the discrete spectrum and the continuous spectrum associated with the singularity of the Rayleigh equation. The continuous spectrum associated with the unbounded domain can also be well predicted by the three methods, even though the Chebyshev tau predictions are somewhat more sensitive to the mapping parameter in the square-root transformation. The global eigensolution methods studied here may be applied very efficiently to obtain either an approximation to the complete eigenvalue spectrum or initial guesses for a local shooting procedure for the discrete part of the spectrum.

REFERENCES

1. L. Rayleigh, "On the Stability, or Instability of Certain Fluid Motions," *Proc. London Math. Soc.*, **11**, pp. 57–70 (1880).

2. A. Michalke, "On the Spatially Growing Disturbances in an Inviscid Shear Layer," *J. Fluid Mech*, **23**, pp.521–544 (1965).

3. M. G. Macaraeg, "A Mixed Pseudospectral/Finite Difference Method for the Axisymmetric Flow in a Heated, Rotating Spherical Shell" *J. Comp. Phys.*, **162**, pp. 297–320 (1986).

4. H. C. Ku and D. Hatziavramidis, "Chebyshev Expansion Methods for the Solution of the Extended Graetz Problem," *J. Comp. Phys.*, **56**, pp. 495-512 (1984).

5. T. A. Zang and M. Y. Hussaini, "Mixed Spectral-Finite Difference Approximations for Slightly Viscous Flows," *Proceedings of the Seventh International Conference on Numerical Methods in Fluid Dynamics*, Ed. Reynolds, W. C., MacCormack, R. W., Springer-Verlag (1981).

6. J. P. Drummond, M. Y. Hussaini and T. A. Zang, "Spectral Methods for Modeling Supersonic Chemically Reacting Fluid Fields,"AIAA paper 85-0302 (1985).

7. S. A. Orszag and G. S. Patterson, "Numerical Simulation of Three-dimensional Homogeneous Isotropic Turbulence," *Phys. Rev. Lett.*, **28**, pp. 76–79 (1972).

8. C. Canuto, M. Y. Hussaini, A. Quarteroni and T. A. Zang, etd., **Spectral Methods in Fluid Dynamics**, Springer-Verlag (1987).

9. S. A. Orszag, "Accurate Solution of the Orr-Sommerfeld Stability Equation," *J. Fluid Mech.*, **50**, pp. 689–703 (1971).

10. T. J. Bridges and P. J. Morris, "Differential Eigenvalue Problems in which the Parameter Appears Nonlinearly," *J. Comp. Phys.*, **55**, pp. 437–460 (1984).

11. R. D. Joslin and P. J. Morris, "The Sensitivity of Flow and Surface Instabilities to Changes in Compliant Wall Properties," *J. Fluid and Structures*, **3**, pp. 423–437 (1989).

12. M. Gaster, E. Kit and I. Wygnanski, "Large-scale Structures in a Forced Turbulent Mixing Layer," *J. Fluid Mech.*, **150**, pp. 23–39 (1985).

13. R. A. Petersen and M. M. Samet, "On the Preferred Mode of Jet Instability," *J. Fluid Mech.*, **194**, pp. 153–173 (1988).

14. W. W. Liou, 'Weakly Nonlinear Models for Turbulent Free Shear Flows', Ph.D. Thesis, Department of Aerospace Engineering, The Pennsylvania State University (1990).

15. L. Fox and I. B. Parker, **Chebyshev Polynomials in Numerical Analysis**, Oxford Univ. Press (1968).

16. W. W. Liou, "The Computation of Reynolds Stress in an Incompressible Plane Mixing Layer," M.S. Thesis, Department of Aerospace Engineering, The Pennsylvania State University (1986).

17. R. G. Voiget, D. Gottlieb and M. Y. Hussaini, ed., **Spectral Methods for Partial Differential Equations**, SIAM (1984).

18. P. G. Drazin and W. H. Reid, **Hydrodynamic Stability**, Cambridge University Press (1981).

19. J. E. Dennis, J. F. Traub and R. P. Weber, "Algorithms for Solvent of Matrix Polynomial," SIAM, *J. Numer. Anal.*, **15**, pp 523–533 (1978).

20. P. Lancaster, "Algorithms for Lambda-Matrices," *Num. Math.*, **6**, pp. 388–394 (1964).

21. C. E. Grosch and S. A. Orszag, "Numerical Solution of Problems in Unbounded Regions: Coordinate Transformations," *J. Comp. Phys.*, **25**, pp. 273–295 (1977).

22. J. P. Boyd, "The Optimization of Convergence for Chebyshev Polynomial Methods in an Unbounded Domain," *J. Comp. Phys.*, **45**, pp. 43–79 (1982).

23. S. A. Orszag, "Spectral Methods for Problems in Complex Geometries," *J. Comp. Phys.*, **37**, pp. 70–92 (1980).

24. K. M. Case, "Stability of Inviscid Plane Couette Flow," *Phys. Fluids*, **3**, pp. 143–148 (1960).

REPORT DOCUMENTATION PAGE	*Form Approved* *OMB No. 0704-0188*

1. AGENCY USE ONLY (*Leave blank*)	2. REPORT DATE	3. REPORT TYPE AND DATES COVERED
	August 1991	Technical Memorandum

4. TITLE AND SUBTITLE
A Comparison of Numerical Methods for the Rayleigh Equation in Unbounded Domains

5. FUNDING NUMBERS
WU-505-62-21

6. AUTHOR(S)
W.W. Liou and P.J. Morris

7. PERFORMING ORGANIZATION NAME(S) AND ADDRESS(ES)
National Aeronautics and Space Administration
Lewis Research Center
Cleveland, Ohio 44135-3191

8. PERFORMING ORGANIZATION REPORT NUMBER
E-6476

9. SPONSORING/MONITORING AGENCY NAMES(S) AND ADDRESS(ES)
National Aeronautics and Space Administration
Washington, D.C. 20546-0001

10. SPONSORING/MONITORING AGENCY REPORT NUMBER
NASA TM-105179
ICOMP-91-13
CMOTT-91-4

11. SUPPLEMENTARY NOTES
W.W. Liou, Institute for Computational Mechanics in Propulsion and Center for Modeling of Turbulence and Transition, NASA Lewis Research Center (work funded by Space Act Agreement C-99066-G). P.J. Morris, Pennsylvania State University, Department of Aerospace Engineering, University Park, Pennsylvania 16802. Space Act Monitor: Louis A. Povinelli, (216) 433-5818.

12a. DISTRIBUTION/AVAILABILITY STATEMENT
Unclassified - Unlimited
Subject Category 64

12b. DISTRIBUTION CODE

13. ABSTRACT *(Maximum 200 words)*
A second-order finite difference and two spectral methods including a Chebyshev tau and a Chebyshev collocation method have been implemented to determine the linear hydrodynamic stability of an unbounded shear flow. The velocity profile of the basic flow in the stability analysis mimicks that of a one-stream free mixing layer. Local and global eigenvalue solution methods are used to determine individual eigenvalues and the eigenvalue spectrum, respectively. The calculated eigenvalue spectrum includes a discrete mode, a continuous spectrum associated with the equation singularity and a continuous spectrum associated with the domain unboundedness. The efficiency and the accuracy of these discretization methods in the prediction of the eigensolutions of the discrete mode have been evaluated by comparison with a conventional shooting procedure. Their capabilities in mapping out the continuous eigenvalue spectra are also discussed.

14. SUBJECT TERMS
Spectral methods; Finite difference; Linear hydrodynamic stability; Global eigensolution methods; Eigenvalue spectrum; Unbounded domain

15. NUMBER OF PAGES
34

16. PRICE CODE
A03

17. SECURITY CLASSIFICATION OF REPORT	18. SECURITY CLASSIFICATION OF THIS PAGE	19. SECURITY CLASSIFICATION OF ABSTRACT	20. LIMITATION OF ABSTRACT
Unclassified	Unclassified	Unclassified	

NSN 7540-01-280-5500

Standard Form 298 (Rev. 2-89)
Prescribed by ANSI Std. Z39-18
298-102